Structure of crystallographically challenged hydrogen storage materials using the atomic pair distribution function analysis

H. Kim,[1] K. Sakaki,[1] K. Asano,[1] M. Yamauchi,[2] A. Machida,[3] T. Watanuki,[3] and Y. Nakamura [1]

[1] Energy Technology Research Institute, National Institute of Advanced Science and Technology, Tsukuba, Ibaraki 305-8565, Japan

[2] Department of Chemistry, Kyushu University, Fukuoka, 812-8581, Japan

[3] Quantum Beam Science Directorate, Japan Atomic Energy Agency, Sayo, Hyogo 679-5148, Japan

Summary

Modern scientifically interesting functional materials are heavily disordered, nano-sized or nano-structured. Although obtaining structural information is an essential part for understanding their fascinating properties, because of their poorly defined Bragg peaks, it is hard to obtain detailed structural information by only using the conventional crystallography method. Here, we apply the atomic pair distribution function (PDF) analysis, a powerful local structural probing technique, to study the hydrogenation process of Pd nanoparticles and the recrystallization process of Pr-rich $Mg_{2-x}Pr_xNi_4$ amorphous hydrides.

key words:

Hydrogen storage materials, local structure, Pd nanoparticles, AB_2 Laves phase

1. Objectives

Structure of Pd hydride nanoparticles

Nano-sized materials, such as nanoparticles, often show quite different properties from their bulk form. Palladium, a well known classical hydrogen-absorbing metal, is not an exception. Yamauchi et al. studied the hydrogen storage properties of polymer-coated Pd nanoparticles with the average diameter of ~2.6 and 7 nm and found that their pressure-composition isotherm (PCT) curves are quite different from that of bulk [1]. As the size gets smaller, the plateau, where Pd-H solid solution and hydride phases coexist, becomes narrower and more tilted and the plateau pressure becomes lower. In addition, the Pd-H solid solution range gets extended. Such alterations in hydrogen storage properties can be explained by the core-shell model. A large number of atoms sitting on the surface lose hydrogen occupation sites and in a hydride phase the atomic arrangement of the first few layers under the surface layer (the shell part) is probably different from that of the core part [2]. The fraction of the shell and the core parts varies with the particle size and it will affect the hydrogen capacity as well as phase transformation behavior i.e. the shape of the PCT curves. In order to get structural information of palladium hydride nanoparticles in more detail, we carried out the in-situ synchrotron X-ray total scattering experiments at various hydrogen contents for the atomic pair distribution function (PDF) analysis [3].

Recrystallization of hydrogen induced amorphous $Mg_{2-x}Pr_xNi_4H_{\sim 6}$ (x=1.2 and 1.4)

Hydrogen induced amorphization (HIA) is a phenomenon that crystalline materials transform into amorphous by absorbing hydrogen. HIA has been reported in many intermetallic compounds including C15 Laves-type AB_2. For C15 Laves phases, there is a well known empirical rule for HIA: when the atomic size ratio, R_A/R_B is greater than 1.37, HIA normally occurs [4]. $Mg_{2-x}Pr_xNi_4$ has a C15b Laves phase structure and R_A/R_B (in our case, R_A is a weighted mean radius of Mg and Pr) exceeds 1.37 when x>1 (Pr-rich composition). As expected, HIA was observed in Pr-rich composition from X-ray diffraction studies using Cu Kα radiation (laboratory X-ray) [5]. From our earlier x-ray and neutron PDF study weakening of correlation between H and the second nearest neighbored Ni was evident in Pr-rich $Mg_{2-x}Pr_xNi_4$ amorphous hydride samples suggesting their heavily distorted metal frame. In this time, we tried to see how amorphous hydride samples recrystallize by heating under vacuum. By studying the recovery process of long-range structural order in amorphous $Mg_{2-x}Pr_xNi_4H_{\sim 6}$ we will have much clear idea of how the metal frame distorted in the amorphous phase.

2. Methods

3.9 nm and 4.5 nm Pd nanoparticles as well as bulk Pd powder samples were packed in in-situ gas loading sample holders and pressurized at various H_2 gas pressures. Amorphous $Mg_{0.8}Pr_{1.2}Ni_4H_{\sim 5}$ and $Mg_{0.6}Pr_{1.4}Ni_4H_{\sim 6}$ samples heated at 300 and 350°C, respectively, for different time intervals were packed in kapton capillaries with a diameter of 1.0 mm. Data were collected at BL22XU at SPring-8 [6] with an incident X-ray energy of 69.85 keV (λ=0.1775 Å) at room temperature using RA-PDF setup [7]. An image plate detector (R-AXISV from Rigaku) was mounted orthogonal to the incident beam with a sample-to-detector distance of 300 mm. The signal from an empty container (a kapton capillary) was subtracted from the raw data, and various other corrections were made [3]. The X-ray PDFs were obtained using the program PDFgetX2 [8]. For local structural studies the PDFgui program [9] was used for real space modeling.

3. Results and Discussion

Pd nanoparticles: Figure 1(a) and (b) show the synchrotron X-ray diffraction patterns of bulk Pd and 4.5 nm Pd nanoparticle, respectively, at various H_2 gas pressures. Diffraction peaks shifted to lower-2θ regions with increasing H_2 gas pressure clearly indicate the occurrence of a solid solution to hydride phase transition in both samples. Note the broadened peaks in 4.5 nm Pd nanoparticle data due to the particle size effect. In Figure 2, the X-ray PDFs of bulk Pd and 4.5 nm and 3.9 nm Pd nanoparticles are plotted. Compared to the bulk Pd PDF, both nanoparticle PDFs show fast decaying of PDF peaks with increasing *r* and the PDF signals disappear above 50 Å due to the finite size effect. The PDF refinement results using one or two face-centered cubic (fcc) structural models are summarized in Table 1. The PDFs of all samples at the absorption plateau (in the two phase region) were well explained by two fcc models. From the difference between two lattice parameters of the fcc models, we can speculate the relative width of the absorption plateau. Difference between refined lattice parameters becomes smaller with decreasing the particle size indicating narrowing of the plateau width. Furthermore, the value of the smaller lattice parameter (a_1) increases with decreasing the particle size reflecting the expansion of the solid solution range in nanoparticle samples. Further analysis is underway.

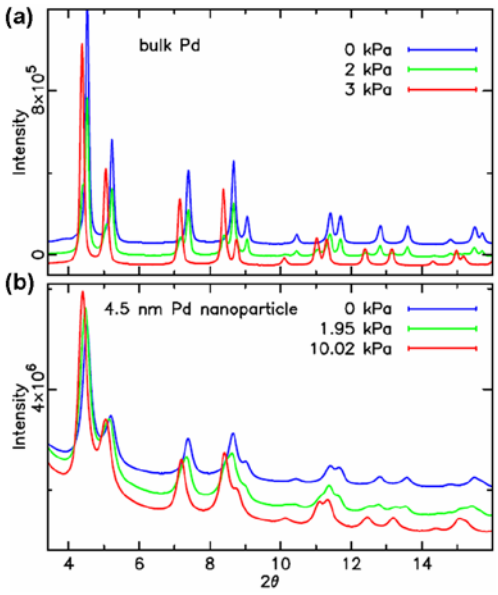

Figure 1. X-ray diffraction patterns of (a) bulk Pd and (b) 4.5 nm Pd nanoparticle at various H_2 gas pressures.

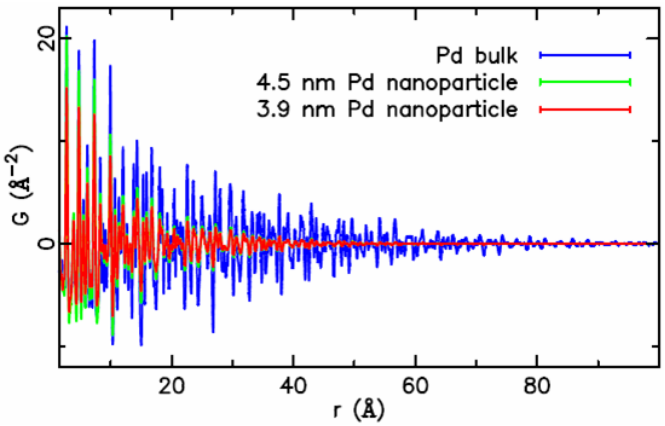

Figure 2. X-ray PDFs of bulk Pd and 4.5 nm and 3.9 nm Pd nanoparticle at 0 kPa of H_2 gas pressure.

Table 1. PDF refinement results using a fcc structural model. The refinement range was $1.7 \leq r \leq 20$ Å. ss, a and f_i indicate solid solution, lattice parameter (Å) and the fraction of phase i, respectively.

phase	Bulk Pd		4.5 nm Pd nanoparticle		3.9 nm Pd nanoparticle	
solid solution phase	0 kPa	a= 3.8957 (metal)	0 kPa	a= 3.9040 (ss)	0 kPa	a= 3.9031 (ss)
two phase region	2 kPa	a_1= 3.8987, a_2= 4.0162	1.95 kPa	a_1= 3.9149, a_2= 3.9991	2.01 kPa	a_1= 3.9186, a_2= 4.0026
		f_1:f_2=0.71:0.29		f_1:f_2=0.6:0.4		f_1:f_2=0.41:0.59
hydride phase	3 kPa	a= 4.0282	10.02 kPa	a= 4.0063	0.1 MPa	a=4.0207

Recrystallization of hydrogen induced amorphous $Mg_{2-x}Pr_xNi_4H_{\sim 6}$ (x=1.2 and 1.4): X-ray PDFs of $Mg_{0.8}Pr_{1.2}Ni_4H_{\sim 5}$ and $Mg_{0.6}Pr_{1.4}Ni_4H_{\sim 6}$ samples heated for different time periods are shown in Figure 3 and 4,

respectively. With increase in heating time the development of mid-to-long range structural order in $Mg_{0.6}Pr_{1.4}Ni_4H_{\sim 6}$ is evident from the features appearing above 10 Å in the PDFs (Figure 4). For $Mg_{0.8}Pr_{1.2}Ni_4H_{\sim 5}$ sample 5 min of heating reduces the overall PDF peak height and shift them to lower-*r*. This is probably because hydrogen is released from the small amount of a Mg-rich crystal phase remaining in the amorphous $Mg_{0.8}Pr_{1.2}Ni_4H_{\sim 5}$. 10 min of heating makes the PDF peaks shifted further to lower-*r* and sharper, especially peaks below 20 Å, indicating the development of mid-range structural order while releasing hydrogen probably from the amorphous phase. More detailed analysis is underway.

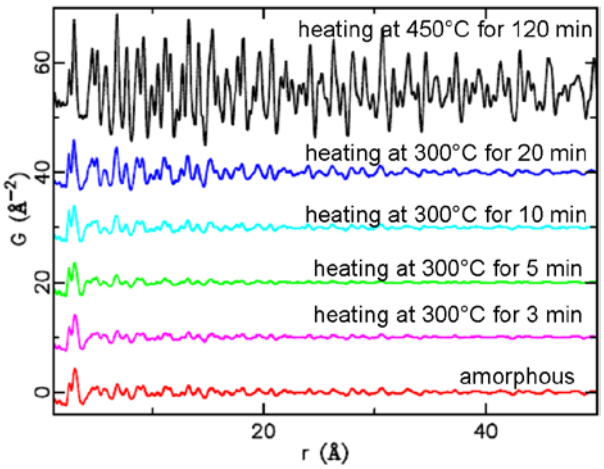

Figure 3. X-ray PDFs of $Mg_{0.8}Pr_{1.2}Ni_4H_{\sim 5}$ heated at 300°C for different time.

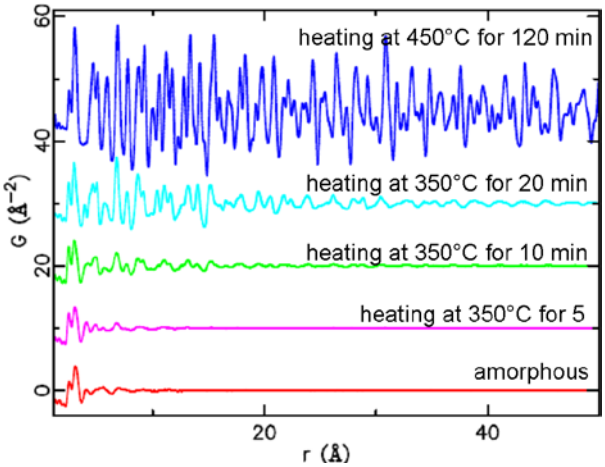

Figure 4. X-ray PDFs of $Mg_{0.6}Pr_{1.4}Ni_4H_{\sim 6}$ heated at 350°C for different time.

4. References

[1] M. Yamauchi et al. *J. Phys. Chem. C* **112**, 3294-3299 (2008).

[2] C. Sachs et al. *Phys. Rev. B* **64**, 075408 (2001).

[3] T. Egami and S. J. L. Billinge, *Underneath the Bragg Peaks: Structural Analysis of Complex Materials*: Pergamon Press Elsevier: Oxford, England, 2003.

[4] K. Aoki *Mater. Sci. Eng. A* **304-306**, 45-53 (2001).

[5] N. Terashita et al. *Mat*. *Trans*. **53**, 513-517 (2012).

[6] T. Watanuki et al., Philos. Mag. **87**, 2905-2911 (2007).

[7] P. J. Chupas et al., J. Appl. Cryst. **36**, 1342-1347 (2003).

[8] Qiu, X.; Thompson, J. W.; Billinge, S. J. L. J. Appl. Crystallogr. **37**, 678 (2004).

[9] Farrow, C. L.; Juhas, P.; Liu, J. W.; Bryndin, D.; Božin, E. S.; Bloch, J.; Proffen, Th.; Billinge, S. J. L. J. Phys.: Condens. Matter **19**, 335219 (2007).